CMLS, Cell. Mol. Life Sci. 62 (2005) 355–361
1420-682X/05/030355-07
DOI 10.1007/s00018-004-4477-1

CMLS Cellular and Molecular Life Sciences

Research Article

The N-terminus of HIV-1 Tat protein is essential for Tat-TAR RNA interaction

O. Chaloin[a, *], J.-C. Peter[a], J.-P. Briand[a], B. Masquida[b], C. Desgranges[c], S. Muller[a] and J. Hoebeke[a]

[a] UPR 9021, Institut de Biologie Moléculaire et Cellulaire, CNRS, 15 rue René Descartes, 67084 Strasbourg (France), e-mail: o.chaloin@ibmc.u-strasbg.fr
[b] UPR 9002, Institut de Biologie Moléculaire et Cellulaire, CNRS, 67084 Strasbourg (France)
[c] UPR 2228, CNRS, UFR Biomédicale des Saints-Pères, 75270 Paris (France)

Received 29 October 2004; received after revision 19 November 2004; accepted 30 November 2004

Abstract. The human HIV transactivator protein Tat is essential for efficient viral transcription that occurs by a complex mechanism involving interaction of Tat with the TAR RNA element. This interaction appears to require the mediation of a cellular protein, cyclin T1. However, the possibility that Tat and TAR associate in a binary Tat-TAR complex has been little investigated. Using a chemically synthesized active Tat protein, the kinetic and equilibrium parameters of its interaction with TAR were determined by surface plasmon resonance technology. Independently of partner and method of immobilization onto the sensor chip, the association ($k_a = 5–9 \times 10^5\ M^{-1}\ s^{-1}$) and dissociation rate constants ($k_d = 1.7–4.3 \times 10^{-3}\ s^{-1}$) yielded similar equilibrium dissociation constants (K_d = 2–8 nM). A truncated peptide encompassing residues 30–86 of Tat did not bind to TAR at all. We conclude that Tat can form a high-affinity complex with TAR in the absence of cyclin T1 and that the N-terminal domain of Tat is essential for this interaction, suggesting a conformational link between this domain and the basic domain of Tat. These results are important in our quest for developing therapeutic compounds that impair viral replication.

The human immunodeficiency virus type 1 (HIV-1) transactivator protein Tat is critical for productive virus replication [1]. Tat is an 86- to 101-amino-acid (aa) protein [2] with varying C termini depending on virus isolate. Tat can be subdivided into several regions: the N terminal comprising residues 1–21, a cysteine-rich domain (aa 22–37), a sequence-conserved hydrophobic core (aa 38–48), a highly basic region (aa 49–59) containing a nuclear localization signal, a glutamine-rich sequence (aa 60–72), and the C-terminal region (aa 73–101) containing an RGD motif. While the first three regions constitute the activation domain, the basic region encompasses an RNA-binding domain that contains an important arginine-rich motif. Tat binds to the so-called TAR RNA, a 59-base stem-loop structure located at the 5′ end of all nascent HIV-1 transcripts [3]. The TAR region 19–42 reproduces the complete activity of the entire TAR RNA. This domain contains the trinucleotide bulge (nucleotides 23–25), which is necessary for high-affinity and specific binding to the Tat protein [4]. The loop region of TAR (nucleotides 30–35) is required for in vivo transactivation but is not involved in binding to Tat [5].

The chemical synthesis of Tat is not an easy task and for this reason, several groups have worked on truncated peptides to study Tat-TAR interactions [6]. However, recent results obtained from molecular dynamics simulations on the HIV-1 Z2 Tat variant [7] have highlighted the relevance of working with the entire Tat protein. The authors identified intramolecular interactions that could be important for stabilizing the structure of Tat between the N terminus and the basic domain of the protein.

* Corresponding author.

Tat protein can also be produced using recombinant DNA methods. While such preparations may be useful to study certain biological effects of Tat, they are less suitable for physico-chemical characterizations due to bacterial and cellular impurities, and potentially impaired folding of the protein. To overcome these problems, we have decided to optimize a solid-phase synthesis protocol to produce and fold properly a pure product on a relatively large scale (100-mg range). We then used this chemically synthesized Tat protein (sTat) to study its interaction to TAR by an electrophoretic mobility shift method, and to determine the physico-chemical parameters of Tat-TAR interaction by surface plasmon resonance.

Materials and methods

Oligonucleotide synthesis

TAR RNA containing 30 bases (5′-GACCAGAUUUGAGCCUGGGAGCUCUCUGGC-3′), the biotinylated-TAR RNA, and the O1 RNA (5′-CCCAGAUUGAGCGCUCUCUGG-3′) used as control were purchased from Dharmacon Research (Lafayette, COL). Biotin was incorporated at the 5′ end during the synthesis. RNAs were purified by electrophoresis on a 15% denaturing polyacrylamide gel. After desalting the pure samples, were aliquoted, lyophilized and kept at –20 °C.

Tat synthesis

Tat protein and biotinylated Tat protein (Biot-Tat) were obtained using the native chemical ligation method introduced by Dawson et al. [8]. The amino-terminal segment Tat [1–21]-α-thioester was prepared on a thioester-generating resin using Boc chemistry and solid-phase peptide synthesis [9]. After completion of chain assembly, the peptide was deprotected and cleaved from the resin using anhydrous hydrogen fluoride containing 10% *p*-cresol for 1 h at 0 °C. Peptide [22–86]Tat from the HIV-1 Lai strain was assembled using optimized Fmoc chemistry protocols with a multichannel peptide synthesizer [10]. Side-chain deprotection and cleavage of peptides from the solid support was performed by treatment with reagent K (82.5% TFA v/v, 5% phenol w/v, 5% water v/v, 5% thioanisole v/v, 2.5% 1,2-ethanedithiol v/v) for 150 min at 20 °C [11].

Tat [1–21]-α-thioester and [22–86]Tat fragments were purified by reversed-phase HPLC (RP-HPLC) using a Beckman preparative HPLC system (Gagny, France) on a Nucleosil C18 (1 × 30 cm) and a Nucleosil C4 (1 × 30 cm) column, respectively (Macherey Nagel, Hoerdt, France). The elution was achieved with a linear gradient of aqueous 0.1% TFA (A) and 0.08% TFA in 80% acetonitrile, 20% water (B) at a flow rate of 6 ml/min with UV detection at 230 nm. The purity of Tat [1–21]-α-thioester and [22–86]Tat fragments was controlled by analytical RP-HPLC on a Beckman instrument (Gagny, France) with a Nucleosil C18 5 µm column (150 × 4.6 mm) and a Nucleosil C4 5 µm column (150 × 4.6 mm), respectively, using a linear gradient of 0.1% TFA in water and acetonitrile containing 0.08% TFA at a flow rate of 1.2 ml/min. The integrity of each peptide was assessed by matrix-assisted laser desorption and ionization time-of-flight (MALDI-TOF) spectrometry on a Protein TOF mass spectrometer (Bruker, Wissembourg, France).

Purified peptide segments Tat [1–21]-α-thioester and [22–86]Tat were dissolved in 6 M guanidine HCl and 0.1 M sodium phosphate, pH 7.5, at a concentration of 3 mM. The pH was monitored and adjusted to 7.5 with 1 M NaOH, and benzylmercaptan 1% v/v and thiophenol 3% v/v were added. After 24 h, the reaction was completed and the ligation product was purified on a Nucleosil C4 (1 × 30 cm) RP-HPLC using the same conditions as described above for the segment [22–86]. The HPLC profile of sTat is shown in figure 1A. The mass of [1–86]Tat was assessed by LC/MS using a Thermo Finigan LCQ

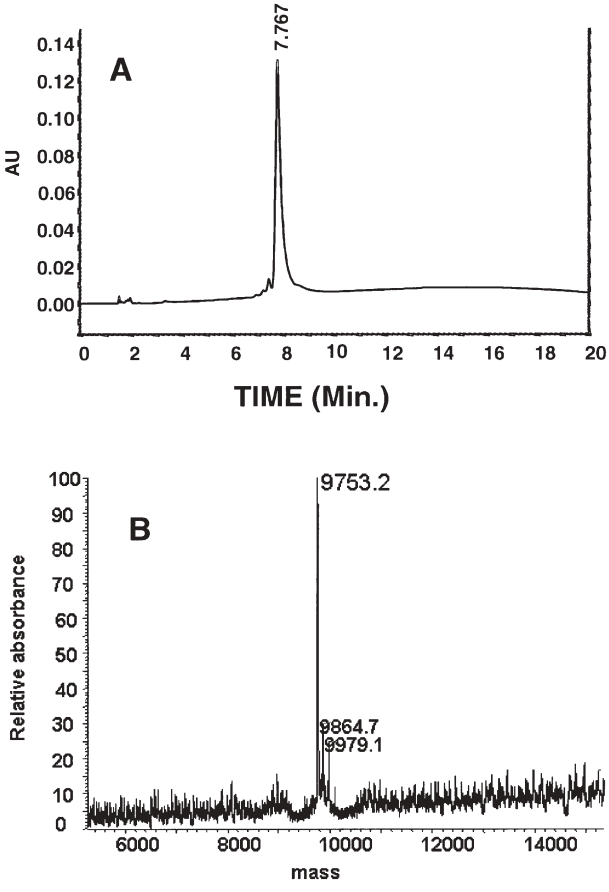

Figure 1. Characterization of the synthetic sTat protein. (*A*) HPLC profile of Tat Lai after purification. Gradient from 5 to 65% B (CH3CN, 0.08% TFA) in 20 min, column C4, 1.2 ml/min, 220 nm; purity: 98%. (*B*) Mass spectrum of [1–86]Tat Lai. MW calculated: 9751.6, MW measured: 9753.2 (M+1).

advantage/LC surveyor (Les Ulis, France) as shown in figure 1B. Tat samples were stored lyophilized at –20 °C to prevent oxidation.

Biot-[30–86]Tat, [44–61] Tat as well as a 21-residue-long peptide called G21V peptide used as control were assembled using Fmoc chemistry, purified and analyzed as described above.

The sequence of all the synthetic compounds is shown in table 1.

Transactivation assays

Transactivation was assayed by inducing Tat-dependent chloramphenicol acetyltransferase (CAT) production in HeLa cells harboring an integrated HIV-1 LTR-CAT gene construct (HL3T1 cells). HL3T1 cells were seeded into a 24-well plate (4×10^4 cells/well) and incubated in Dulbecco's modified Eagle's medium (DMEM) (Invitrogen, Cergy Pontoise, France) complemented with 10% fetal calf serum (FCS). Active recombinant Tat protein (a gift from Aventis Pasteur, Lyon, France) was diluted in DMEM-10% FCS (final volume 500 µl) supplemented with 100 µM chloroquine (Sigma Sanitquentin Fallarien, France) to final concentrations of 125–1000 ng/ml. The solutions were then added to the cells and incubated for 24 h. Then the cells were washed twice with PBS and incubated in fresh DMEM-10% FCS for an additional 24 h. Finally, cells were lysed and CAT production was assayed with a CAT ELISA kit (Roche Diagnostics, Meylan, France) following the manufacturer's instructions.

Electrophoretic mobility shift assays

The oligoribonucleotides (biotinylated or not) were dissolved in HBS (10 mM HEPES, 150 mM NaCl, 34 mM EDTA, pH 6.5) at a final concentration of 1 mM, incubated for 1 min at 70 °C and immediately cooled at 4 °C. Then, 2 µl of a 10 µM solution of TAR RNA was incubated with 4 µl of a 10 µM solution of freshly dissolved Tat protein in HBS for 10 min on ice. Then, 1 µl of loading dye solution (MBI Fermantas, Mundolsheim, France) was added to 10 µl of the Tat/TAR mixture and 10µl (100 pmol TAR and 200 or 400 pmol Tat) was loaded on a 4% agarose gel (with ethidium bromide). The electrophoresis buffer was 40 mM Tris-HCl pH 8.0, containing 20 mM acetic acid and 1 mM EDTA.

Biosensor experiments

The BIACORE 3000 system, sensor chip CM5, surfactant P20, amine coupling kit containing N-hydroxysuccinimide (NHS) and N-ethyl-N′-dimethylaminopropyl carbodiimide (EDC), 2-(2-pyridinyl-dithioethaneamine) (PDEA) were from BIACORE (Uppsala, Sweden). Streptavidin was obtained from Sigma. All biosensor assays were performed with HBS as running buffer (20 mM HEPES, 20 mM sodium acetate, 140 mM potassium acetate, 3 mM magnesium acetate, 0.02% surfactant P20, pH 7.3). The oligoribonucleotides and the peptides were dissolved in the running buffer. The peptide G21V was used as control. The sensor chip surface was regenerated after each experiment by injecting 10 µl of 100 mM H_3PO_4.

RNA and protein immobilization on the streptavidin-coated chip

Immobilization of streptavidin was performed by injecting onto the surface activated with EDC/NHS of a sensor chip CM5, 35 µl streptavidin (100 µg/ml in 50 mM formate buffer, pH 4.3), which gave a signal of approximately 5000 RU, followed by 20 µl ethanolamine hydrochloride, pH 8.5, to saturate the free activated sites of the matrix. Biotinylated TAR, Biot-Tat protein and Biot-[30–86]Tat fragment (100 µg/ml in HEPES buffer) were allowed to interact with streptavidin until a response of approximately 40, 4900 and 3600 RU, respectively, was obtained.

Table 1. Sequences of synthetic peptides and proteins.

Name	Sequence	MW calculated	MW measured (M+1)
Tat	Nle[1]EPVDPRLEPWKHPGSQPKTACTTCYCKKC-CFHCQVCFTTKALGISYGRKKRRQRRRPPQGS-QTHQVSLSKQPTSQPRGDPTGPKE[86]	9751.60	9753.2
Biot-Tat	BiotNle[1]EPVDPRLEPWKHPGSQPKTACTTCYCK-KCCFHCQVCFTTKALGISYGRKKRRQRRRPPQ-GSQTHQVSLSKQPTSQPRGDPTGPKE[86]	9977.92	9978.0
Biot-[30–86]Tat	BiotC[30]CFHCQVCFTTKALGISYGRKKRRQRRR-PPQGSQTHQVSLSKQPTSQPRGDPTGPKE[86]	6681.70	6682.6
[44–61]Tat	G[44]ISYGRKKRRQRRRPPQG[61]	2196.55	2197.8
G21V	GIIDLIEKRKFNQNSNSTYCV	2442.77	2443.4

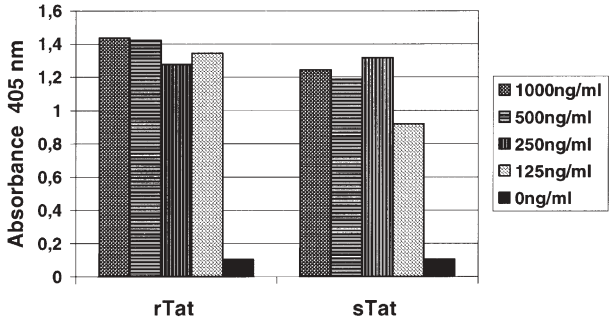

Figure 2. Transactivation assays with recombinant Tat (rTat) and synthetic Tat (sTat). rTat and sTat at four concentrations (125–1000 ng/ml) were used in a transactivation assay (see Materials and methods). The results are expressed as absorbance values at 405 nm.

Protein immobilization by the cysteine method

Peptide G21V (800 RU) and Tat protein (5200 RU) were immobilized through thiol groups of the cysteine residues using 35 µl PDEA in 50 mM borate buffer pH 8.3 on the NHS/EDC-activated matrix. Then, 35 µl of peptides (100 µg/ml in formate buffer, pH 4.3) were injected until a response of approximately 800 and 5200 RU, respectively, was obtained. Finally, 20 µl of 50 mM cysteine, 1 M NaCl solution was used to saturate the unoccupied sites on the chip.

Kinetic measurements

All the binding experiments were carried out at 25 °C with a constant flow rate of 30 µl/min. Before starting experiments, we verified that peptide [30–86]Tat had no binding affinity to RNA TAR. The results (see fig. 5B) demonstrated that peptide [30–86]Tat could be used as a control for our experiments.

For the first series of experiments, Biot-TAR was immobilized on the sensor chip and different concentrations of [30–86]Tat and Tat (1.25–10 nM) were injected for 5 min, followed by a dissociation phase of 5 min.

For the second series of experiments, Tat protein and G21V peptide were immobilized via the thiol group of the cysteine residues onto the sensor chip and different concentrations of TAR (2.5–20 nM) were injected for 5 min, followed by a dissociation phase of 6 min.

For the third series of experiments, Biot-[30–86] fragment and Biot-Tat protein were immobilized on the sensor chip and different concentrations of TAR (2.5–20 nM) were injected for 5 min, followed by a dissociation phase of 5 min.

In the three series of experiments, the sensor chips were regenerated with a 30 s flux of 100 mM H_3PO_4. The kinetic parameters were calculated using the BIAeval 3.1 software on a personal computer. Analysis was performed using the simple Langmuir binding model. The specific binding profiles were obtained after subtracting the response signal from the peptide control. The fitting to each model was judged by the chi-square value and randomness of residue distribution compared to the theoretical model.

Results

As shown in figure 1, the Tat protein prepared by chemical ligation was obtained at a high purity (above 95%) and perfectly characterized by mass spectrometry. To ascertain that the chemically synthesized Tat was also biologically active, we used a transactivation assay to compare it with recombinant Tat (rTat). As shown in figure 2 both Tat preparations showed similar activity.

To check the ability of the two protagonists Tat and TAR to interact in solution, a gel mobility shift assay was performed on a 4% agarose gel. In an equimolar ratio, the migration of TAR oligonucleotide was not retarded (data not shown). However, the migration of TAR RNA (or Biot-TAR RNA, fig. 3A) was retarded in a dose-dependent manner in the presence of Tat protein in a 1:2 and 1:4 molar ratio (see Materials and methods) (fig. 3B). Tat and

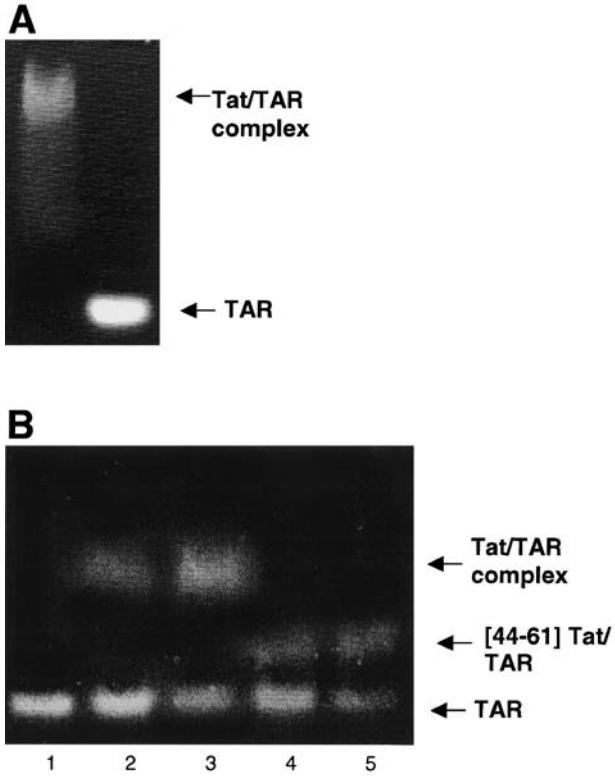

Figure 3. Gel mobility shift assay. (*A*) Biot-Tat and TAR-biot in a molecular ratio 2:1 are able to form a complex with an aberrant migration profile (left compared to TAR alone, right). (*B*) Tat and TAR and a Tat fragment (residues 44–61) are also able to complex together. Lane 1, TAR alone; lane 2, TAR and Tat in a molecular ratio 2:1; lane 3, TAR and Tat in a molecular ratio 1:4; lane 4, TAR and [44–61]Tat in a molecular ratio 2:1; lane 5, TAR and [44–61]Tat in a molecular ratio 4:1.

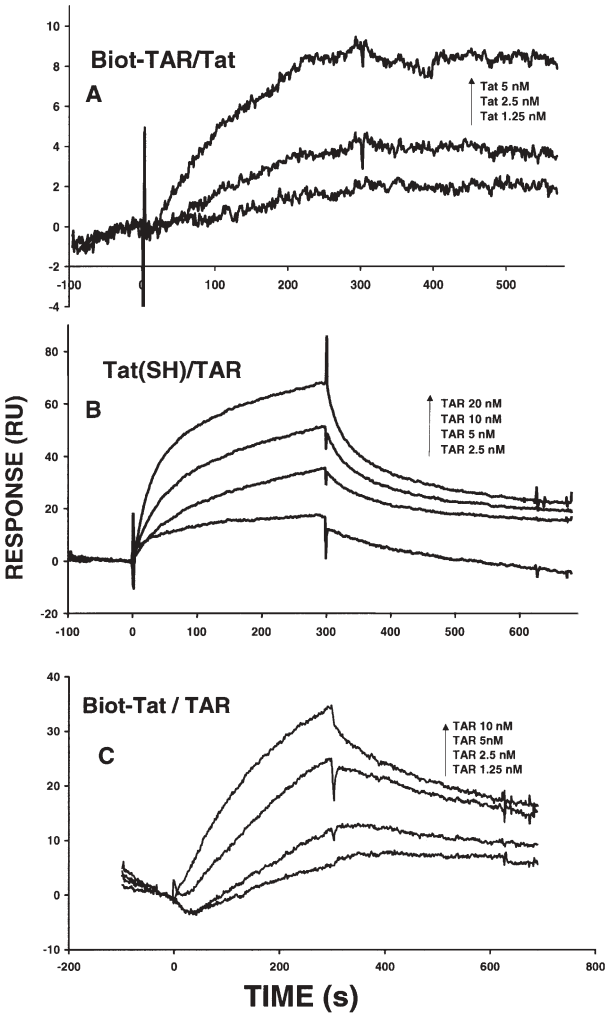

Figure 4. Sensorgrams of the binding of TAR to Tat tested in different test formats. (*A*) Sensorgrams of the binding of sTat to the Biot-TAR RNA immobilized on streptavidin. (*B*) Sensorgrams of the binding of TAR to sTat immobilized via the thiol groups of the cysteine residues. (*C*) Sensorgrams of the binding of TAR to sTat immobilized on streptavidin.

TAR were able to form a complex, migrating more slowly in the gel because of the difference in molecular mass and charge, without the presence of a third partner.

We therefore decided to study the physico-chemical parameters of the bimolecular interaction using surface plasmon resonance technology. In a first series of experiments, we immobilized biotinylated TAR RNA on the sensor chip, and different concentrations of sTat were used as the analyte in the running buffer. For each concentration, the association and dissociation curves were fitted separately. The sensorgrams and the fitting parameters are summarized in figure 4 and table 2. The results indicate that Tat binds to TAR with a fast association and a slow dissociation rate constant ($5.50 \times 10^5\ M^{-1}\ s^{-1}$ and $4.30 \times 10^{-3}\ s^{-1}$). The dissociation equilibrium constant (K_d) indicates a high binding affinity between TAR and sTat (7.8 nM).

In a second series of experiments, the synthetic protein Tat was used as the ligand immobilized by the thiol groups of the cysteine-rich sequence. In this case, non-biotinylated TAR RNA was used as the analyte at different concentrations. Control experiments were carried out with the non-Tat-related G21V peptide (for its sequence, see table 1). The sensorgrams and the fitting parameters are summarized in figure 4 and table 2. As expected, the fitting results indicate that TAR RNA binds to sTat with association and dissociation rate constants comparable to those measured in the format described above, namely, $6.03 \times 10^5\ M^{-1}$ s-1 for the association rate constant and $4.04 \times 10^{-3}\ s^{-1}$ for the dissociation rate constant. The K_d value (6.7 nM) confirms that even though Tat was immobilized onto the sensor chip by its cysteine residues, sTat and TAR interact with a high binding affinity.

To confirm these results, in the last series of experiments, we immobilized a biotinylated form of sTat protein through streptavidin onto the sensor chip and the TAR RNA was used at different concentrations as the analyte in the running buffer.

In this series of experiments, we also included a control with the oligonucleotide O1, lacking the binding bulge of TAR, to check the specificity of the interaction with the protein Tat at 100 nM. As shown in figure 5A, no interaction between Tat and the oligonucleotide O1 was detectable even at a high concentration of O1 RNA.

For each concentration, the association and dissociation curves were fitted separately using a simple Langmuir model. The sensorgrams and the fitting parameters are summarized in figure 4 and table 2. In complete agreement with the results described above, the fitted results indicate that TAR RNA binds to sTat with a fast association rate and a slower dissociation rate constant ($9.22 \times 10^5\ M^{-1}\ s^{-1}$ and $1.70 \times 10^{-3}\ s^{-1}$). The K_d value measured in this

Table 2. Kinetic parameters of Tat-TAR interactions k_a, kinetic association rate; k_d, kinetic dissociation rate; K_a, equilibrium association constant; K_d, equilibrium dissociation constant; R_{max} (RU), maximal response expressed as resonance units. χ^2, chi square value.

Ligand	Analyte	k_a ($M^{-1}\ s^{-1}$)	k_d (s^{-1})	K_a (M^{-1})	K_d (M)	R_{max} (RU)	χ^2
Biot-TAR	Tat	5.51×10^5	4.29×10^{-3}	1.28×10^8	7.79×10^{-9}	15.4	0.08
Tat	TAR	6.03×10^5	4.04×10^{-3}	1.49×10^8	6.71×10^{-9}	69.8	3.73
Biot-Tat	TAR	9.22×10^5	1.70×10^{-3}	5.42×10^8	1.85×10^{-9}	37.8	2.07

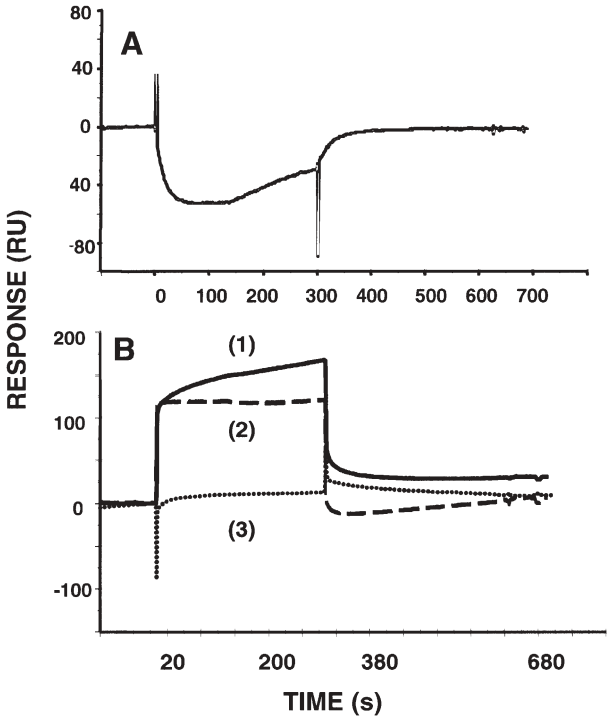

Figure 5. (*A*) Sensorgram in the presence of 100 nM O1 RNA with immobilized Tat. (*B*) Sensorgrams of the binding of 10 nM TAR to Biot-Tat (curve 1), to Biot-[30–86]Tat (curve 2) and with the buffer (curve 3). The fast increase at t0 is due to the difference of refractive index between the solubilizing and the running buffers.

set of experiments (1.9 nM) supports our conclusion that sTat and TAR interact with a high binding affinity in the absence of cyclin T1.

Discussion

Interaction between Tat and TAR is one of the essential processes involved in HIV replication [12]. Recent observations suggested that a high-affinity interaction between Tat and TAR is necessarily mediated by a third partner, cyclin T1, to form a stable complex [13, 14]. Furthermore, acetylation of Tat on Lys^{50} was shown to allow the formation of a Tat-TAR complex but to inhibit the interaction with cyclin T1 [15]. However, all these binding studies were performed by electrophoretic mobility shift experiments that are suitable for qualitative investigations but do not allow the precise determination of physico-chemical parameters of Tat-TAR interaction. To circumvent this difficulty, interaction experiments have been performed using fragments derived from the Tat protein [16, 17], with the risk that the determined parameters do not reflect the interaction of the whole protein with TAR. Since we were able to chemically synthesize the entire Tat protein in a pure and biologically active form, we studied its interaction with TAR using surface plasmon resonance.

We first confirmed by an electrophoretic mobility test that sTat protein was able to form a stable complex with TAR in the absence of cyclin T1 [see also ref. 5]. This is in contrast with previous findings [13, 14, 18] and could be due to the fact that compared to the chemically synthesized sTat, rTat protein used in the previous studies adopts a different conformation in solution. This may also be due to agents used for its purification and solubilization, or to contaminating side-products present in the Tat preparation that can readily interact with rTat protein. In general, recombinant Tat is produced in *Escherichia coli* as a glutathione S-transferase fusion protein. rTat can be easily cleaved from the fusion protein and purified by thrombin proteolytic digestion. However, these different steps may affect its conformation and stability.

The findings obtained from the electrophoretic mobility shift experiments were confirmed by surface plasmon resonance measurements. To exclude any possible artefacts due to the immobilization of one or another of the partners onto the sensor chip, three different set-ups were used: (i) biotinylated TAR was immobilized on a streptavidin matrix, (ii) sTat protein was linked by one or more of its SH groups, and (iii) sTat protein was immobilized via a biotin moiety introduced at its N terminus to streptavidin immobilized on the chip. Under these three conditions, similar kinetic and affinity parameters were obtained (table 2), and indicated a high-affinity complex at a nanomolar range between Tat and TAR. The K_d values were very close to those measured previously by filter binding assays [5]. While the dissociation rate constants were of the same magnitude as those observed for Tat basic peptide-TAR interactions, the association rate constants were a thousand times faster, yielding nanomolar equilibrium dissociation constants instead of micromolar equilibrium dissociation constants as previously determined [17]. The conformation of the entire Tat protein seems thus to favor interaction kinetics of the protein to TAR.

Interestingly, when a biotinylated N terminus deletion fragment of Tat was used as ligand, namely the fragment [30–86], no binding to TAR could be detected (fig. 5B), suggesting the importance of the N-terminal domain for this interaction. These results may explain the low-affinity binding of TAR and Tat peptides corresponding to the basic region of the Tat protein [17]. They also strengthen the conclusions drawn from molecular dynamics simulations [7] suggesting an interaction between the N-terminal Asp2 and Lys51 and Arg53 in the basic region of Tat. The biological relevance of this interaction was assessed by site-directed mutagenesis. Changing the negative charge at position 2 of Tat dramatically altered its biological activity [7]. This could be due to loss of high-affinity binding to TAR. In good agreement with these conclusions, recent results have shown that anti-Tat monoclonal antibodies directed to the N terminus or to

the basic region of Tat inhibited the accumulation of extracellular Tat in the cytoplasm and nuclei of Jurkat cells, and considerably reduced viral replication in vitro [19, 20].

In conclusion, we have demonstrated that chemically synthesized Tat protein interacts with TAR with high affinity (nanomolar range) in the absence of cyclin T1 and that this interaction requires the N terminus of the Tat protein. The methodology described in this work might prove useful for the high-throughput screening discovery of novel inhibitors of the Tat-TAR interaction.

Acknowledgements. This study was supported by CNRS. O. C. was supported by a fellowship from SIDACTION.

1 Cullen B. R. (1986) Trans-activation of human immunodeficiency virus occurs via a bimodal mechanism. Cell **46:** 973–982
2 Jeang K. T., Xiao H. and Rich E. A. (1999) Multifaceted activities of the HIV-1 transactivator of transcription, Tat. J. Biol. Chem. **274:** 28837–28840
3 Rana T. M. and Jeang K. T. (1999) Biochemical and functional interactions between HIV-1 Tat protein and TAR RNA. Arch. Biochem. Biophys. **365:** 175–185
4 Churcher M. J., Lamont C., Hamy F., Dingwall C., Green S. M., Lowe A. D. et al. (1993) High affinity binding of TAR RNA by the human immunodeficiency virus type-1 tat protein requires base-pairs in the RNA stem and amino acid residues flanking the basic region. J. Mol. Biol. **230:** 90–110
5 Dingwall C., Ernberg I., Gait M. J., Green S. M., Heaphy S., Karn J. et al. (1990) HIV-1 tat protein stimulates transcription by binding to a U-rich bulge in the stem of the TAR RNA structure. EMBO J. **9:** 4145–4153
6 Darfeuille F., Arzumanov A., Gryaznov S., Gait M. J., Di Primo C. and Toulme J. J. (2002) Loop-loop interaction of HIV-1 TAR RNA with N3′-P5′ deoxyphosphoramidate aptamers inhibits in vitro Tat-mediated transcription. Proc. Natl. Acad. Sci. USA **99:** 9709–9714
7 Pantano S., Tyagi M., Giacca M. and Carloni P. (2004) Molecular dynamics simulations on HIV-1 Tat. Eur. Biophys. J. **33:** 344–351
8 Dawson P. E., Muir T. W., Clark-Lewis I. and Kent S. B. (1994) Synthesis of proteins by native chemical ligation. Science 266: 776–779
9 Hojo H. and Aimoto S. (1991) Polypeptide synthesis using the S-alkyl thioesther of a partially protected peptide segment: synthesis of the DNA binding domain of c-Myb protein (142–193)-NH2. Bull. Chem. Soc. Japan **64:** 111–117
10 Neimark J. and Briand J. P. (1993) Development of a fully automated multichannel peptide synthesizer with integrated TFA cleavage capability. Peptide Res. **6:** 219–228
11 King D., Fields C. and Fields G. (1990) A cleavage method which minimizes side reactions following Fmoc solid-phase peptide synthesis. Int. J. Peptide Protein Res. **36:** 255–266
12 Jones K. A. and Peterlin B. M. (1994) Control of RNA initiation and elongation at the HIV-1 promoter. Annu. Rev. Biochem. **63:** 717–743
13 Wei P., Garber M. E., Fang S-M., Fisher W. H. and Jones K. A. (1998) A novel CDK9-associated C-type cyclin interacts directly with HIV-1 Tat and mediates its high-affinity, loop-specific binding to TAR RNA. Cell **92:** 451–462
14 Richter S., Cao H. and Rana T. M. (2002) Specific HIV-1 RNA loop sequence and functional groups are required for human cyclin T1-Tat-TAR ternary complex formation. Biochemistry **41:** 6391–6397
15 Kaehlcke K., Dorr A., Hetzer-Egger C., Kiermer V., Henklein P., Schnoelzer M. et al. (2003) Acetylation of Tat defines a cyclin T1-independent step in HIV transactivation. Mol. Cell **12:** 167–176
16 Long K. S. and Crothers D. M. (1995) Interaction of human immunodeficiency virus type 1 tat-derived peptides with TAR RNA. Biochemistry **34:** 8885–8895
17 Tassew N. and Thompson M. (2003) Kinetic characterization of TAR RNA-Tat peptide and neomycin interactions by acoustic wave biosensor. Biophys. Chem. **106:** 241–252
18 Wimmer J., Fujinaga K., Taube R., Cujec T. P., Zhu Y., Peng J. et al. (1999) Interactions between Tat and TAR and human immunodeficiency virus replication are facilitated by human cyclin T1 but not cyclins T2a or T2b. Virology **255:** 182–189
19 Tikhonov I., Ruckwardt T. J., Hatfield G. S. and Pauza C. D. (2003) Tat-neutralizing antibodies in vaccinated macaques. J. Virol. **77:** 3157–3166
20 Moreau E., Hoebeke J., Zagury D., Muller S. and Desgranges C. (2004) Generation and characterization of neutralizing human monoclonal antibodies against human immunodeficiency virus type 1 Tat antigen. J. Virol. **78:** 3792–3796